PCCP

Pushing the limits of the electrochemical window with pulse radiolysis in chloroform

Journal:	*Physical Chemistry Chemical Physics*
Manuscript ID	CP-ART-04-2020-001948.R1
Article Type:	Paper
Date Submitted by the Author:	04-Jun-2020

Complete List of Authors:	Bird, Matthew; Brookhaven National Laboratory, Chemistry Department Cook, Andrew; Brookhaven National Laboratory, Chemistry Department Zamadar, Matibur; Stephen F Austin State University, Chemistry and Biochemistry Asaoka, Sadayuki; Kyoto Institute of Technology, Department of Biomolecular Engineering Miller, John; Brookhaven National Laboratory,

ARTICLE

Pushing the limits of the electrochemical window with pulse radiolysis in chloroform

Received 00th January 20xx,
Accepted 00th January 20xx

DOI: 10.1039/x0xx00000x

Matthew J. Bird,*[a] Andrew R. Cook, [a] Matibur Zamadar,[b] Sadayuki Asaoka[c] and John R. Miller [b]

Pulse radiolysis (PR) enables the full redox window of a solvent to be accessed, as it does not require electrodes or electrolyte which limit the potentials accessible in voltammetry measurements. PR in chloroform has the additional possibility to enable reaching highly positive potentials because of its large ionization potential (IP). PR experiments demonstrated the formation of the (deuterated) chloroform radical cation $CDCl_3^{+\bullet}$, identifying it as the source of the broad absorption in the visible part of the spectrum. Results indicated that solutes with a redox potential up to +3.7 V vs Fc/Fc^+ can be oxidized by $CDCl_3^{+\bullet}$, which is far beyond what is possible with electrochemical techniques. Oxidation is not efficient because of rapid geminate recombination with chloride counterions, but also due to rapid decomposition of $CDCl_3^{+\bullet}$ which limits the yield of otherwise longer-lived free ions. The rapid, 6 ± 3 ns, decomposition, confirmed by two independent experiments, means that a solute must be present at a concentration >100 mM to capture >90% of the free holes formed. Addition of ethene removes the broad, overlapping absorptions from ubiquitous (chlorine atom, solute) complexes created by PR in halogenated solvents enabling clear observation of solute cations. The results also unravel the complex radiation chemistry of chloroform including the large reported value $G(-CHCl_3)$ = 12 molecules/100 eV for the decomposition of chloroform molecules.

Introduction

Pulse radiolysis (PR) is well-known to readily form radical cations of molecules and study them with high time resolution. Electrochemical techniques often are unable to determine oxidation potentials for molecules with high ionization potentials.[1, 2] or to examine properties of their radical cations. In principle PR in solvents having high IP's might be expected to do this well, but limitations are often encountered. This paper describes PR of deuterated chloroform ($CDCl_3$), which like many other halogenated solvents will only produce oxidizing species following pulse radiolysis (PR).[3] Chloroform is an excellent solvent for many organic molecules, including conjugated polymers of great current interest in organic photovoltaic and light emitting diode applications, facilitating investigation of their radical cations.[4-6] At high concentration, solutes can be oxidized faster than diffusion with PR which is useful for studying fast hole transport processes or short-lived cations.[6] The large ionization potential of chloroform (experimental gas phase, IP_{exp} = 11.37 eV[7]) also should enable oxidation of high IP solutes to their radical cations. If PR in chloroform could form the radical cation of any molecule with an IP_{exp} < 11.37 eV, it could push well past the limits of known electrochemical windows (< +3V vs SCE)[1, 2, 8] for determining oxidation potentials. Why has such an ability not been demonstrated? Earlier studies[4, 9-11] have often found that PR in chloroform falls short of its expected abilities, but the complicated long history of this subject has yet to fully illuminate why or to clarify the details of the nature, yield and lifetime of the oxidizing species. Here we seek to understand why chloroform PR has not become a richer tool for oxidizing molecules and find ways to take advantage of its capabilities, starting with an in-depth review of the literature.

Ionization of liquid chloroform creates electrons and holes (eqn 1). The ejected electron is captured by another solvent molecule which can then undergo mesolytic cleavage creating a chloride ion and $CHCl_2^\bullet$ radical (eqn 2). There is debate over the existence and lifetime of the chloroform radical anion. A proposed assignment of an absorption band at 470 nm to the radical anion $CHCl_3^{-\bullet}$ in methylcyclohexane[12] would imply it has a lifetime of ~40 ns at room temperature. We, and others,[5, 6, 11, 13] however have yet to see evidence of solute radical anions formed in liquid chloroform following radiolysis suggesting dissociative electron capture by the solvent. We also note a similar diversity of findings in CCl_4 with reports of radical anion lifetimes ranging from fs[14] through to ps[15] and ns.[16] Oxidation of solutes observed following PR in chloroform is attributed to the hole, the radical cation $CHCl_3^{+\bullet}$, or possibly from neutral radicals.[11] The low dielectric constant (ε_r = 4.8) of $CHCl_3$ suggests that many ionizations will result in coulombically bound ion pairs that decay via geminate

[a] Chemistry Department, Brookhaven National Laboratory, Upton, New York 11793, USA.
[b] Department of Chemistry and Biochemistry, Stephen F. Austin State University, Nacogdoches, Texas 75962-3006, USA.
[c] Department of Biomolecular Engineering, Kyoto Institute of Technology, Matsugaskaki, Sakyo-ku, Kyoto 606-8585, Japan.
Electronic Supplementary Information (ESI) available: [details of any supplementary information available should be included here]. See DOI: 10.1039/x0xx00000x

recombination (eqn 3), leaving a low yield of free ions and a large concentration of $CHCl_2^{\bullet}$ and reactive $Cl^{\bullet}$ atoms.

$CHCl_3 \rightsquigarrow CHCl_3^{+\bullet} + e^{-\bullet}$ (1)
$e^{-\bullet} + CHCl_3 \rightarrow CHCl_3^{-\bullet} \rightarrow CHCl_2^{\bullet} + Cl^-$ (2)
$CHCl_3^{+\bullet} + Cl^- \rightarrow CHCl_3^* + Cl^{\bullet}$ (3)
$CHCl_3^* \rightarrow$ fragments $(CHCl_2^{\bullet},Cl^{\bullet}),(CCl_3^{\bullet},H^{\bullet}),(CCl_2, HCl)$ (4)

While we have not found a reported value, we might expect a free ion yield, G_{fi}, of 0.1 – 0.5 ions/100 eV based on solvents of similar dielectric constant from the compiled values of G_{fi} by Allen.[17] Results below will explain why G_{fi} has been difficult to measure. Assuming dissociative capture, eqn 2, an upper limit for *all* ions (free and geminate) can be inferred from reported yields of the primary neutral radicals $CHCl_2^{\bullet}$ and $Cl^{\bullet}$ based on eqns 2 and 3. In a 1982 review[18] Adabie attempted to reconcile conflicting G-values for these primary radicals from Werner and Firestone,[19] and others.[20-26] Variations arise due to detection of different products and different views on how to relate them to primary radicals, as well as strong dose-rate dependence and interference from stabilizers such as ethanol.[18] In one detail, we favor the reasoning of Ottolenghi[26], Baxter[20] and Bibler[21] who do not find a plausible mechanism for $Cl^{\bullet}$ to be responsible for the formation of CCl_4, whose yield is independent of dose rate and radical scavengers. With this approach, the literature values can be summarized as $G(Cl^{\bullet}) = 4.6$[19] and 4.8 ± 0.1[26] and $G(CHCl_2^{\bullet}) = 4.8$.[19], 5.0 [20,21] and 5.9 ± 0.4.[26] We therefore expect a plausible $G(CHCl_3^{+\bullet})_{max}$ ~4.8 ± 0.2 ions/100 eV, which is an upper limit because some $CHCl_2^{\bullet}$ and $Cl^{\bullet}$ radicals could be made by direct excitation, without ionization, followed by eqn 4.

The two radicals $CHCl_2^{\bullet}$ and $Cl^{\bullet}$ can either react with the solvent to produce $CCl_3^{\bullet}$ (equations 5 and 6), leading to equal amounts of CH_2Cl_2 and C_2Cl_6 (equations 5-7) or with each other (most significantly at high dose rates or in spurs[27]) to make $C_2H_2Cl_4$ and C_2HCl_5 (equations 8-9). Other products exist, notably CCl_4, but these four halocarbons were found to account for 87% of decomposed $CHCl_3$ molecules[19] for which the value is $G(-CHCl_3) = 12$ molecules / 100 eV at room temperature[22] which can be traced to eqns 2, 4, 5 and 6.

$CHCl_2^{\bullet} + CHCl_3 \rightarrow CH_2Cl_2 + CCl_3^{\bullet}$ (5)
$Cl^{\bullet} + CHCl_3 \rightarrow CCl_3^{\bullet} + HCl$ (6a)
$Cl^{\bullet} + CDCl_3 \rightarrow CCl_3^{\bullet} + DCl$ (6b)
$2CCl_3^{\bullet} \rightarrow C_2Cl_6$ (7)

$2CHCl_2^{\bullet} \rightarrow C_2H_2Cl_4$ (8)
$CHCl_2^{\bullet} + CCl_3^{\bullet} \rightarrow C_2HCl_5$ (9)

We hypothesize that these reactions are affected little by H/D isotope effects except when CH or CD bonds are broken (e.g eq 6). Equations 1 – 4 do not fully explain the initial radiolysis of chloroform because the formation of CCl_4 is yet to be explained; understanding its origin is closely linked to the goals of this paper. Invariance of $G(CCl_4)$ to dose rate[21] suggests a radical-radical pathway is unlikely and a lack of CCl_4 in vapor phase radiolysis[20] implies that the surrounding solvent molecules play a role.

A hint of the origin of CCl_4 comes from Baxter's evidence that its yield is reduced by the cation scavengers NH_3 and n-butanol.[20] Baxter reasoned that the CCl_4 yield was derived from some fraction of the solvent cations and thus set a *lower* limit for *all* ions (free and geminate) of $G(CHCl_3^{+\bullet})_{min} = 0.88$ ions/100 eV. Baxter's data also appears to suggest that the mechanism converting the cationic species to CCl_4 occurs fast enough that low concentrations of cation scavengers cannot out-compete it. This was evidenced by the lack of a non-zero intercept in a scavenged yield vs $[scavenger]^{1/2}$ plot which suggests the, normally long-lived, *free* cations have been converted to something else before the scavenger can find them.

Baxter,[20] Burrows[11] and Arai,[3] observed oxidation of solutes in chloroform with microsecond pulse radiolysis, but the identity of the oxidizing species was not clear. G-values for solute cations included 0.53, 1.55, 1.58, and 3.25 ions/100 eV for four different solutes at 10 mM.[11] We seek to solve these mysteries by understanding the fate of the primary chloroform cation.

The first report of transient absorptions in neat chloroform was by Washio in 1983 utilizing picosecond pulse radiolysis.[9] With ~ 100 ps resolution, it was possible to resolve two absorption bands in the neat solvent peaking at 330 nm and 550 nm with lifetimes of ~10 ns and ~1 ns respectively. The narrow UV band was tentatively assigned to $CCl_2^{\bullet}$ and the shorter-lived broad visible band was initially unknown. The author noted that if this 550 nm band were due to $CHCl_3^{+\bullet}$, the kinetics implied additional routes of cation decay other than just recombination with Cl^-. Data below will corroborate this conclusion. The 330 nm band was later shown by Chateauneuf, through experiments in carbon tetrachloride,[28] to be a charge transfer to solvent transition from chlorine atom. Chateauneuf found this species to be common in many chlorinated solvents, and that the position of the band depends on the IP of the solvent.[29] The decay of the 330 nm band is due to hydrogen abstraction from the $CHCl_3$ solvent (eqn 6).

The broad visible absorption peaking ~550 nm has not been conclusively assigned, and there remains considerable disagreement over the species responsible. As noted above, a broad absorption peaked at 470 nm formed during pulse radiolysis of chloroform in methylcyclohexane at -130 C was assigned to the chloroform radical anion by Katsumura.[30] In a later 1989 paper, Washio adopted Katsumura's interpretation to assign the 550 nm band in liquid chloroform to the $CHCl_3^{-\bullet}$.[10] The lack of any reports of solute radical anion formation in liquid chloroform following PR casts some doubt upon the concept of a chloroform radical anion that lives long enough to undergo electron transfer to the solute. A recent study of photodissociation in liquid CCl_4 and $CHCl_3$ has attributed visible bands to be from Cl atom complexes called iso-CCl_3-Cl and iso-$CHCl_2$-Cl, respectively,[31] both of which would have significant charge transfer character. Iso-CCl_3-Cl is similar in spirit to the $CCl_3^+||\ Cl^-$

separated ion pair of Bühler or variations proposed by Washio,[32] Miyasaki[33] or Zhang and Thomas.[34]

Investigating cation formation with transient absorption following PR in chlorinated solvents is difficult because rapid geminate charge recombination of the solute (S) radical cation with the chloride ion often forms either long-lived complexes or ion pairs rather than returning the solute to its original neutral state (eqns 10 and 11 respectively).

$$S^{+\bullet} + Cl^- \rightarrow (S^{\delta+}, Cl^{\delta-}) \quad (10)$$

$$S^{+\bullet} + Cl^- \rightarrow (S^{+\bullet}, Cl^-) \quad (11)$$

The Cl atom in a complex (eqn 10) can be long-lived and have strong absorptions in the visible region[28, 35, 36] that obscure solute cation absorptions[3] making identification of solvent radical cation absorptions and determination of yields difficult. The Cl atom decay via hydrogen abstraction from $CHCl_3$ (eqn 6) occurs with a reported rate constant[37] of 1.4×10^7 $M^{-1}s^{-1}$, giving a lifetime of ~10 ns in neat chloroform. However, in complexes with benzene, CS_2 and pyridine the reactivity of the Cl atom towards hydrogen abstraction is reduced by factors of 160, 420 and 19,000 respectively, increasing lifetimes[36] of such Cl complexes to microseconds or more.

In this paper we establish the yield and kinetics of the parent radical cation and the extent to which side reactions play a role. Deuterated chloroform ($CDCl_3$) was used in all experimental data, because $Cl^\bullet$ had a longer lifetime (see Fig S1a in ESI†) in $CDCl_3$ than $CHCl_3$ (29 ns vs 12 ns), which made it easier to separate out processes happening on different timescales. However, the decay of the visible absorption band following PR, noted to be unusual,[9] is identical in both solvents (S1b in ESI†). The method we adopt is the study of cations formed from solutes with high ionization potentials. We argue that only $CDCl_3^{+\bullet}$ can form radical cations from these molecules. We take care to distinguish the absorption due to radical cations from that due to complexes and find a way to eliminate the Cl atom complex absorptions. The findings presented here enable chloroform to be used as a solvent for making cations by pulse radiolysis in a clear way.

Experimental

Pulse radiolysis was performed using the Laser Electron Accelerator Facility (LEAF) at Brookhaven National Laboratory. For a detailed description of the experimental setup see elsewhere.[38, 39] Photoelectrons from a ~ 3 ps laser pulse striking a magnesium photocathode are accelerated to 9 MeV with a temporal width < 20 ps and typical charge of 5 – 10 nC resulting in typical doses in the range of 10 – 50 Gray. The electron pulse was focused into argon-bubbled solutions in either 2 cm or 0.5 cm path length fused silica cells before being collected by a Faraday cup to allow for correction due to shot to shot dose fluctuations. For measuring spectra or kinetics, light from a pulsed Xenon lamp was focused into the cell counter-collinearly to the electron beam. The transmitted light was then passed through 10 nm-width interference filters before being measured by various detectors depending on the wavelength: silicon (EG&G FND-100Q, <1000 nm, ~1 ns resolution) or InGaAs (GPD Optoelectronics GAP-500L, > 1000 nm, ~5 ns) photodiodes or a biplanar phototube (Hamamatsu R1328U-03, <650 nm, ~200 ps). The detector output was digitized with a LeCroy Waverunner 640Zi oscilloscope (4 GHz bandwidth).

Experiments with ~ 15 ps time resolution used the Optical Fiber Single-Shot (OFSS) detection system, providing single-shot electron pulse-laser probe transient absorption[39] where the time resolution is limited mostly by the width of the electron pulse. This method was used for single wavelengths in the region 580 - 950 nm.

The following solutes were used as received: 2,4,6-Tris(trifluoromethyl)-1,3,5-triazine (Alfa Aesar), 2,4,6-tris(heptafluoropropyl)-1,3,5-triazine (Alfa Aesar), hexachloroethane (Aldrich), fumaronitrile (Aldrich), 1,2-dichloroethane (Aldrich), carbon tetrabromide (Aldrich), n-pentane (Aldrich), carbon disulfide (Aldrich), hexafluorobenzene (Aldrich), cyclohexane (Aldrich), decane (Aldrich), decafluorobiphenyl (Alfa Aesar), 2,3 dimethyl butane (Phillips), benzene (Aldrich), dicyanobiphenyl (CPL), 4,4''-dinitro-p-terphenyl (Alfa Aesar), biphenyl (Matheson, Coleman and Bell), 4-nitro-p-terphenyl (Aldrich), fluorene (Aldrich), 4,4'' cyanopentylterphenyl (Alfa Aesar), and p-terphenyl (Aldrich).

The deuterated chloroform (Aldrich) had a silver foil stabilizer. Solvents were dried over R5 molecular sieve which also removed the ethanol inhibitor from regular chloroform (Aldrich) that has been known to affect yields.[18]

Results & Discussion

I. Yield and lifetime of primary solvent cation

To probe the primary radical cation formed by pulse radiolysis of $CDCl_3$, we investigated a series of high IP solutes (oxidation potentials approximately +1 to over +4 V vs ferrocene/ferrocenium, see also in section III). We use computed values, IP_{calc}, throughout the following sections due to a lack of a complete set of reliable experimental IP values for all solutes investigated. Calculations were performed for non-deuterated molecules with density functional theory in Gaussian 09[40] using B3LYP/6-31g(d).

Of these solutes, carbon disulfide (IP_{calc} = 10.12 eV) was chosen to probe the total yield of the parent solvent cation because it could be dissolved to a high concentration enabling rapid hole capture, it was one of the highest IP solutes investigated that showed unambiguous cation formation, and it had a clear separation between its cation and Cl atom complex absorption. Calculations shown in section III say that CS_2 can be oxidized only by $CHCl_3^{+\bullet}$ or $CDCl_3^{+\bullet}$ and not any other potential oxidizing species formed by PR in chloroform.

Fig 1a shows transient absorption spectra from a solution of 100 mM CS_2 in $CDCl_3$. According to TD-DFT calculations in the ESI† (Fig S3a) the broad absorption centered around 690

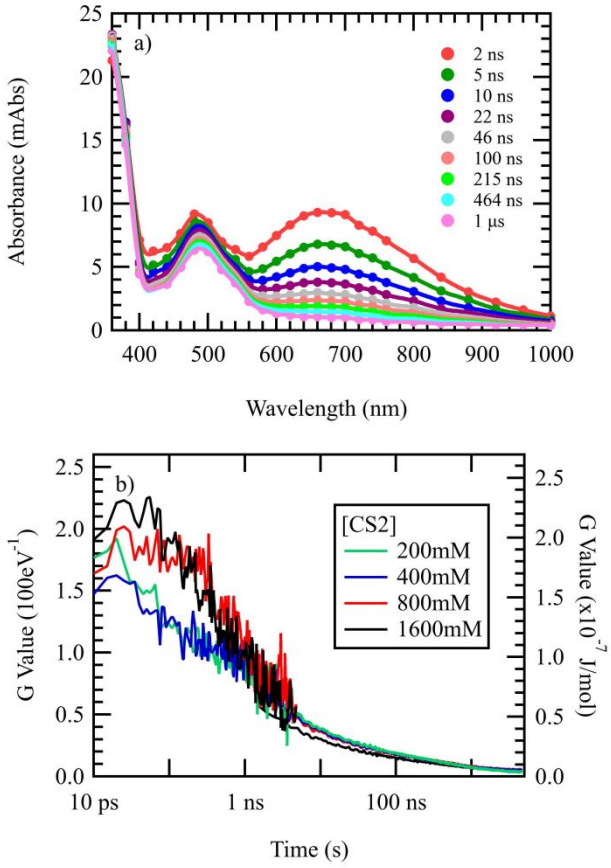

Fig 1 a) Transient absorption spectra following PR of a solution of 100 mM CS_2 in $CDCl_3$ in a 2 cm path length with an average dose of 8.07 Gray b) G-value of cations captured from chloroform by various concentrations of CS_2 following pulse radiolysis of $CDCl_3$. G-values are calculated based on the extinction coefficient of CS_2 dimer cation of 7,775 $M^{-1}cm^{-1}$ at 690 nm (with reference to 15,550 $M^{-1}cm^{-1}$ for the biphenyl radical cation[6] see Fig S2 in ESI†). The doses and pathlengths were 12.5 Gray, 5 mm (OFSS data up to 4 ns) and 41.7 Gray, 2 mm (data beyond 4 ns).

nm is the $(CS_2)_2^{\bullet+}$ dimer radical cation formed by reaction of $CS_2^{\bullet+}$ with CS_2, and the peaks at ~490 nm and < 400 nm are from the Cl atom complex with CS_2.[36, 41] Fig 1b shows transient absorption at 690 nm for a series of CS_2 concentrations in $CDCl_3$ with ~ 15 ps resolution with the Optical Fiber Single-Shot (OFSS) pulse-probe method.[39] Using an extinction coefficient for the dimer cation of 7,775 $M^{-1}cm^{-1}$ (see Fig S2 in ESI†) the y-axes scaling in Fig 1b converts the absorbance to the G-value as a function of time.

The total yield of CS_2 dimer cations at 15 ps was (2.3 ± 0.2) ions/100 eV. This value is a lower limit for the yield of solvent radical cations at t = 0 because geminate charge recombination was occuring at the same time as both hole attachment to CS_2 and the subsequent dimerization to form species we are monitoring.

While observations below will confirm a faster decay, if we were to assume that the $CDCl_3^{+\bullet}$ had a similar decay profile to that seen for $(CS_2)_2^{\bullet+}$ in Fig 1b, then a solute at a concentration as low as 1 mM would have had time to capture all available solvent holes by 500 ns, assuming a typical diffusion controlled rate constant of $1 - 2 \times 10^{10}$ $M^{-1}s^{-1}$. In contrast to this assumption the yield of $(CS_2)_2^{\bullet+}$ ions, observed at 500 ns, drops precipitously for CS_2 concentrations < 100 mM (Fig 2, yellow data).

We estimate that 500 ns is a reasonable choice of time where geminate recombination is largely complete, so mostly *free* ions are observed. Data from Fig 1b show that when all free ions are scavenged, the G-value at 500 ns is 0.1 ions/100 eV which is at the lower end of what might be expected for a free ion yield in a solvent with ε_r = 4.8. Data in Fig S4 in ESI† suggest a more accurate estimate of the free ion yield may be lower, between 0.06 and 0.08 ions/100 eV. This was found by extrapolating the long-lived component of the radical cation transient absorptions to t = 0. Capture of free ions is usually insensitive to solute concentration, so it is surprising that the ion yield at 500 ns is so dependent on solute concentration. When CS_2 is present at 10 mM, about half as many *free* $(CS_2)_2^{\bullet+}$ ions are made as compared to

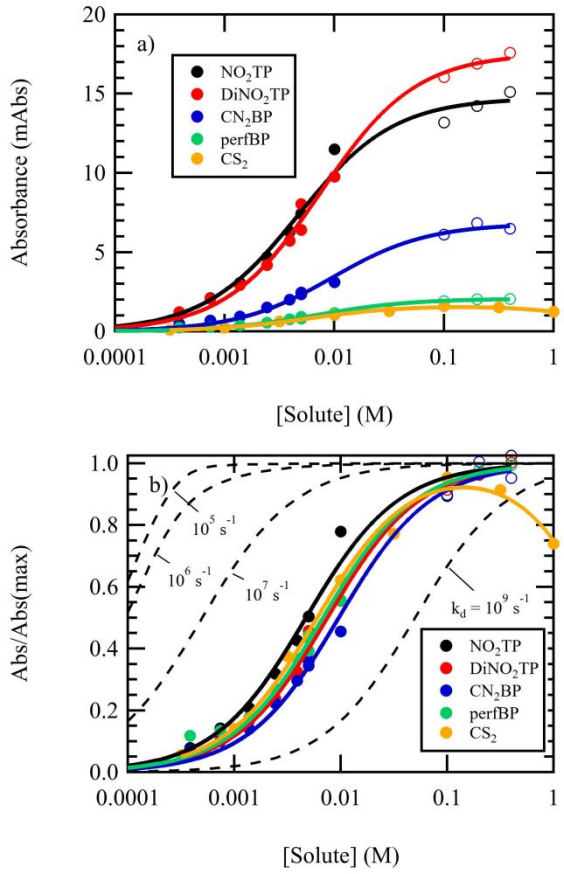

Fig 2 a) Absorbance at 500 ns after the electron pulse for various concentrations of solutes in $CDCl_3$. Solutes and observation wavelengths were: 4-nitro-p-terphenyl (NTP) 1000 nm, 4,4''-dinitro-p-terphenyl (DNTP) 980 nm, 4,4'-dicyanobiphenyl (DCBP) 780 nm, decafluorobiphenyl (F-BP) 900 nm and CS_2 800 nm. b) Traces are normalized to the maximum absorbance estimated from the fit to equation 13. Dashed black lines are for equation 13 plotted with $k_{att} = 2.0 \times 10^{10}$ $M^{-1}s^{-1}$. Tags on the dashed lines indicate the rate constant, k_d, for an additional decay process of the solvent cation but not the solute cation. The solid black line is the best fit to all data while holding k_{att} = 2.0×10^{10} $M^{-1}s^{-1}$ and finds $k_d = 1.25 \times 10^8$ s^{-1}. Colored lines are best fits to individual datasets with $k_d = 1.25 \times 10^8$ s^{-1} and k_{att} allowed to vary. Open circles correspond to [1,2-dichloroethane] with the named solute being at 5 mM.

when [CS_2] = 100 mM. This result implies that the oxidizing species, identified below as $CDCl_3^{+\bullet}$, has a fundamental lifetime that is competitive with the ~5 – 10 ns it should take to oxidize a solute at 10 mM with a diffusion-controlled rate. We characterize this unexplained loss of $CDCl_3^{+\bullet}$ with eqn 12 and a rate constant, k_d.

$$CDCl_3^{+\bullet} \xrightarrow{k_d} \text{unknown species} \quad (12)$$

The rate constant, k_d, may be sensitive to whether the cation is normal $CHCl_3^{+\bullet}$ or deuterated $CDCl_3^{+\bullet}$. To investigate further the lifetime of the parent solvent radical cation, the dependence of the yield of solute cations at 500 ns on the concentration of CS_2 and a range of other solutes was studied; the results are shown in Fig 2a. The solutes, 4-nitro-p-terphenyl (IP_{calc} = 7.78 eV), 4,4''-dinitro-p-terphenyl (IP_{calc} = 8.26 eV), 4,4'-dicyanobiphenyl (IP_{calc} = 8.63 eV) and perfluorobiphenyl (IP_{calc} = 9.25 eV) were chosen because their radical cations have strong absorptions at longer wavelengths which we expected would reduce overlap with absorptions from Cl atom complexes (see Fig S3 in ESI† for TD-DFT spectra). For all these high-IP solutes the yields drop for solute concentrations <100 mM. This ubiquitous behavior rules out a CS_2 monomer to dimer cation equilibrium as the cause for the shape of the plot in Fig 2a. Note that this is not a typical scavenging experiment that captures all cations (geminate and free) at high solute concentrations and only free at low concentrations. Here, we are probing at a point in time where only radical cations (solvent or solute) formed at large distances from the ejected electron have survived annihilation through charge recombination. Solvent cations that otherwise would have existed at 500 ns, should all have had time to oxidize even the lowest concentrations of solutes used here assuming a typical diffusion-controlled electron transfer rate of 1 – 2 × 10^{10} $M^{-1}s^{-1}$.

Fig 2b shows common behavior amongst the various solutes when the absorbances from their radical cations are normalized to the maximum absorbance found when the solute is at a high concentration. The proposed mechanism, that competition between $CDCl_3^{+\bullet}$ decay, k_d (eqn 12), and hole transfer to solutes with a rate constant, k_{att}, controls the yield of solute cations formed, was tested with a model. The resulting eqn 13 is derived in S5 in ESI†. The decay described by k_d is unique to $CDCl_3^{+\bullet}$ but the model also implicitly assumes that, in addition, all radical cations (solute and solvent) have a common rate constant for decay due to recombination with chloride or reacting with an impurity in the solvent.

$$\frac{Abs(Sol^+)(t)}{Abs_{max}(Sol^+)(t)} = \frac{k_{att}[Sol]}{k_d + k_{att}[Sol]}\left[1 - e^{(-k_d - k_{att}[Sol])t}\right]e^{-k_{att}\beta[Sol]t} \quad (13)$$

Eqn 13 gives, as a fraction, the amount of solute radical cations present at some time, t, compared to how many would have been present had the solvent cation not decayed via eqn 12 before passing on the hole. It is a function of the solute concentration, [*Sol*]. The fraction is the absorbance, *Abs*, divided by the maximum absorbance, Abs_{max}, if all the solvent cations were captured, i.e. the limit for when [*Sol*] becomes large. In order to find Abs_{max} for solutes with low solubility, 1-2-dichloroethane (DCE) was used to as a hole mediator. DCE is soluble at high concentrations and once oxidized by the solvent cations it gives an oxidizing species that lives long enough to transfer the hole to the second solute at 5 mM, as shown by the open circles in Fig 2b. Eqn 13 also contains a term to account for decay of the solute cation due to impurities introduced with the solute, which would reduce the concentration of solute cations surviving to 500 ns. This behavior was only observed with CS_2 as the solute and is characterized with some fraction, β, of the solute being an impurity. For other solutes, β = 0.

Using eqn 13, a global fit was performed to find k_d using a universal value of the $CDCl_3^{+\bullet}$ hole transfer rate, k_{att}, but varying $Abs_{max}(Sol^+)(t)$ for each solute. By fixing k_{att} for all fits to a typical diffusion-controlled rate constant of $k_{att} = 2 \times 10^{10}$ $M^{-1}s^{-1}$ we obtain a best fit of $k_d = (1.25 \pm 0.06) \times 10^8$ s^{-1}, giving a $CDCl_3^{+\bullet}$ fragmentation lifetime of ~8 ns. Eqn 13 is plotted as the thick black line in Figure 2b with these parameters. We later show in section IV that k_{att} = 2 × 10^{10} $M^{-1}s^{-1}$ is a reasonable estimate.

The remaining, colored traces in Figs 2a and 2b are where we allow k_{att} to vary in each fit but hold k_d to our best fit value of 1.25 × 10^8 s^{-1}. When allowed to go free the k_{att} values range from 1.3 – 2.6 × 10^{10} $M^{-1}s^{-1}$. The normalized data shown in Fig 2b are shown along with the predicted behavior for different values of k_d to illustrate the common trend for all solutes and how the intrinsic lifetime of the solvent cation could not have been as low as 1 ns or as large as 100 ns.

II. Fragmentation.

Fragmentation of $CD(H)Cl_3^{+\bullet}$ (eqn 12) could explain the mysterious origin of CCl_4,[20] the unusual decay kinetics of the 550 nm absorption band[9] and our observation of needing high solute concentrations to capture all of the free holes from the solvent. Here DFT computations with the default Gaussian09[40] solvent reaction field (SCRF) model for regular chloroform estimated the energetics of various fragmentation reactions to seek insight into what fragmentations might occur. Free energies, G^*_l, for products and reactants were computed at 1 M standard states, following the method of Kelly.[42] We also follow the approach of Kelly[43] for the free energy when one of the reactants is the solvent. Fragmentation to $CHCl_2^+$ (eqn 14) was found to be downhill (exoergic) having a standard free energy change, ΔG^*_l = -198 meV, although an energy vs C-Cl bond length scan suggested a 260 meV barrier (Fig S6a in ESI†). Eqn 15, showing fragmentation to $CCl_2^{+\bullet}$, was overall uphill at standard concentrations (ΔG^*_l = +99 meV) but if modelled as an equilibrium it could conceivably go to completion at micromolar concentration due to entropy.

$$CHCl_3^{+\bullet} \rightarrow CHCl_2^+ + Cl^\bullet \quad (14)$$
$$CHCl_3^{+\bullet} \rightarrow CCl_2^{+\bullet} + HCl \quad (15)$$

Fragmentation reactions become more favorable when surrounding solvent molecules participate as in eqns 16 and 17, which are downhill with ΔG^*_l = -412 meV and -345 meV respectively. HCl might be formed in one step (equation 16) or in a sequential process of fragmentation (equation 14) followed by hydrogen abstraction (equation 6). Either way, if fragmentation occurs, there will be either CCl_3^+ and $CHCl_2^\bullet$, or $CHCl_2^+$ and $CCl_3^\bullet$ formed in close proximity. The hole will likely end up as CCl_3^+ because the calculated oxidation potential of $CCl_3^\bullet$ is lower than that of $CHCl_2^\bullet$ by 67 mV.

$$CHCl_3^{+\bullet} + CHCl_3 \rightarrow CCl_3^+ + CHCl_2^\bullet + HCl \quad (16)$$
$$CHCl_3^{+\bullet} + CHCl_3 \rightarrow CHCl_2^+ + CCl_3^\bullet + HCl \quad (17)$$

These bimolecular fragmentation reactions (eqns 16-17), which result in formation of CCl_3^+, combined with possible recombinations (18 and 19) are appealing because they could explain three mysteries noted so far: 1) how CCl_4 could be derived from some, but not all, cations[20] 2) why CCl_4 is not detected in gas phase radiolysis[20] and 3) the lack of dose rate dependence of CCl_4 formation.[21] Reactions 17 and 19, like reaction 6 may be affected by H/D isotope substitution.

$$CCl_3^+ + Cl^- \rightarrow (CCl_3^+, Cl^-) \rightarrow CCl_4 \quad (18)$$
$$CHCl_2^+ + Cl^- \rightarrow (CHCl_2^+, Cl^-) \rightarrow CHCl_3 \quad (19)$$

There are some hints in the literature that point to an imbalance in the primary yields of $G(CHCl_2^\bullet)$ and $G(Cl^\bullet)$ which could support $CHCl_3^{+\bullet}$ fragmentation. Bibler[21] found that for *homogeneous* (non-spur) radicals, $G(CHCl_2^\bullet)'$ was greater than $G(CCl_3^\bullet)'$ by 0.6 – 1.0 molecules/100 eV (only counting $CCl_3^\bullet$ derived from H-abstraction by $Cl^\bullet$, eqn 6, and not formed from $CHCl_2^\bullet$ itself via eqn 5). This result could imply an additional source of $CHCl_2^\bullet$ which can be explained by eqn 16.

It is possible that an H from $CHCl_3^{+\bullet}$ and a Cl from a neighbouring $CHCl_3$ might occasionally get close enough to form an H-Cl bond making eqn 16 a one-step reaction. The exact energetic barrier for this is hard to compute with simple DFT due to the number of degrees of freedom and potential surfaces. Full ab initio molecular dynamic is beyond the scope of this work, but we show a suggestive DFT scan of the H-Cl bond formation in ESI† fig S6b.

We sought direct evidence of fragmentation by looking for oxidation of solutes by CCl_3^+ and possibly $CDCl_2^+$. Table 1 shows a range of solute IPs both above and below those calculated for $CCl_3^\bullet$ and $CHCl_2^\bullet$. In the low solute concenration regime, this experiment would show an increased yield of solute cations for solutes with a lower IP than $CCl_3^\bullet$ or $CHCl_2^\bullet$ if the intrinsic lifetime of the fragment cations, CCl_3^+ or $CDCl_2^+$**,** is signficantly longer than the parent cation $CDCl_3^{+\bullet}$.

Calculations in Table 1 predict that CCl_3^+ would oxidize fluorene to its radical cation, but similar oxidation might not occur for biphenyl and definitely not for decafluorobiphenyl.

Table 1 Experimental IPs, calculated IPs and calculated oxidation potentials for solutes studied in section II. The table includes possible species relevant to chloroform radical cation fragmentation, whose cations could potentially oxidize solutes with lower oxidation potentials.

Solute	NIST IP (eV)[a]	IP_{calc} in gas phase (eV)[b]	Calc. absolute E° in $CHCl_3$ (V)[c]	Est. E° in $CHCl_3$ vs Fc/Fc+ (V)[d]
Chloroform	11.37	11.11	9.15	4.09
Carbon disulfide	10.07	10.12	8.06	3.00
Decafluorobiphenyl	8.87	9.25	7.62	2.56
CCl_2	-	9.27	7.18	2.12
Dicyanobiphenyl	-	8.63	7.06	2.00
$CCl^\bullet$	-	9.18	6.83	1.77
4,4''-dinitro-p-terphenyl	-	8.26	6.77	1.71
Biphenyl	8.16	7.86	6.42	1.36
4-nitro-p-terphenyl	-	7.78	6.39	1.33
$CHCl_2^\bullet$	-	8.44	6.38	1.32
$CCl_3^\bullet$	-	8.25	6.33	1.27
Fluorene	7.91	7.60	6.19	1.13
4-cyano-4''-n-pentyl-p-terphenyl	-	7.44	6.19	1.13
p-terphenyl	7.80	7.34	6.09	1.03

Table notes: a) From the NIST Chemistry Webbook where "evaluated" values were available.[7] b) IP, being an enthalpy, is calculated at 298 K using ΔH° for $A_{(gas)} \rightarrow A^{+\bullet}_{(gas)} + e^-_{(gas)}$ and uses $H^\circ(e^-_{(gas)})$ = 0.0362 eV at 298 K. c) "Absolute E°" defined using $-\Delta G^\circ/F$ for ΔG° in the following reaction where $A^{+\bullet}_{(sol)} + e^-_{(gas)} \rightarrow A_{(sol)}$ where F is the Faraday constant and $G^\circ(e^-_{(gas)})$ at 1 atm and 298 K is neglected, being reported as ~0.3 meV[44] d) The oxidation potentials vs Fc/Fc+ were scaled from the "absolute E°" column of numbers based on E°(Fc/Fc+) being estimated to be +5.06 V on this scale. This calibration was determined by considering the average shift of calculated values required to best match reported oxidation potentials (vs Fc/Fc+) for biphenyl (1.52 V), naphthalene (1.36 V) and fluorene (1.27 V), all reported in dichloromethane vs Fc/Fc+.[45] Other reported values for the same compounds in 90 % DCM with other additives would give a slightly different calibration.[46] Naphthalene, not shown in the table, was calculated to have an absolute E° of 6.29 V in chloroform.

Experimental tests were not conclusive. Fig 3a shows transient absorption data following PR for three representative solutes probed at wavelengths corresponding to the peaks of their radical cation absorption spectra (see Fig S8 in ESI† for the other solutes from Table 1). The dicyanobiphenyl trace is typical for high IP solutes at 1 mM, showing only decay of the cation, when only a small fraction of solvent cations were captured. The absorption data for two solutes, fluorene and biphenyl, that could potentially be oxidized by CCl_3^+ or $CDCl_2^+$ appear to show a different behaviour. Both solutes show a growth consistent with a diffusion-limited bimolecular reaction with a solute at 1 mM and an apparently larger yield of cations than dicyanobiphenyl. However, while at first glance this may appear to be evidence of oxidation by a fragment cation, the spectra did not resemble the cations of either solute, as seen in Fig 3b for biphenyl (black trace).

The spectrum (black) in Fig 3b is consistent with an earlier report for PR of biphenyl in chloroform.[3] It is not a good match to the known spectrum of biphenyl cation which can be observed clearly in 1,2-DCE, but interestingly not in

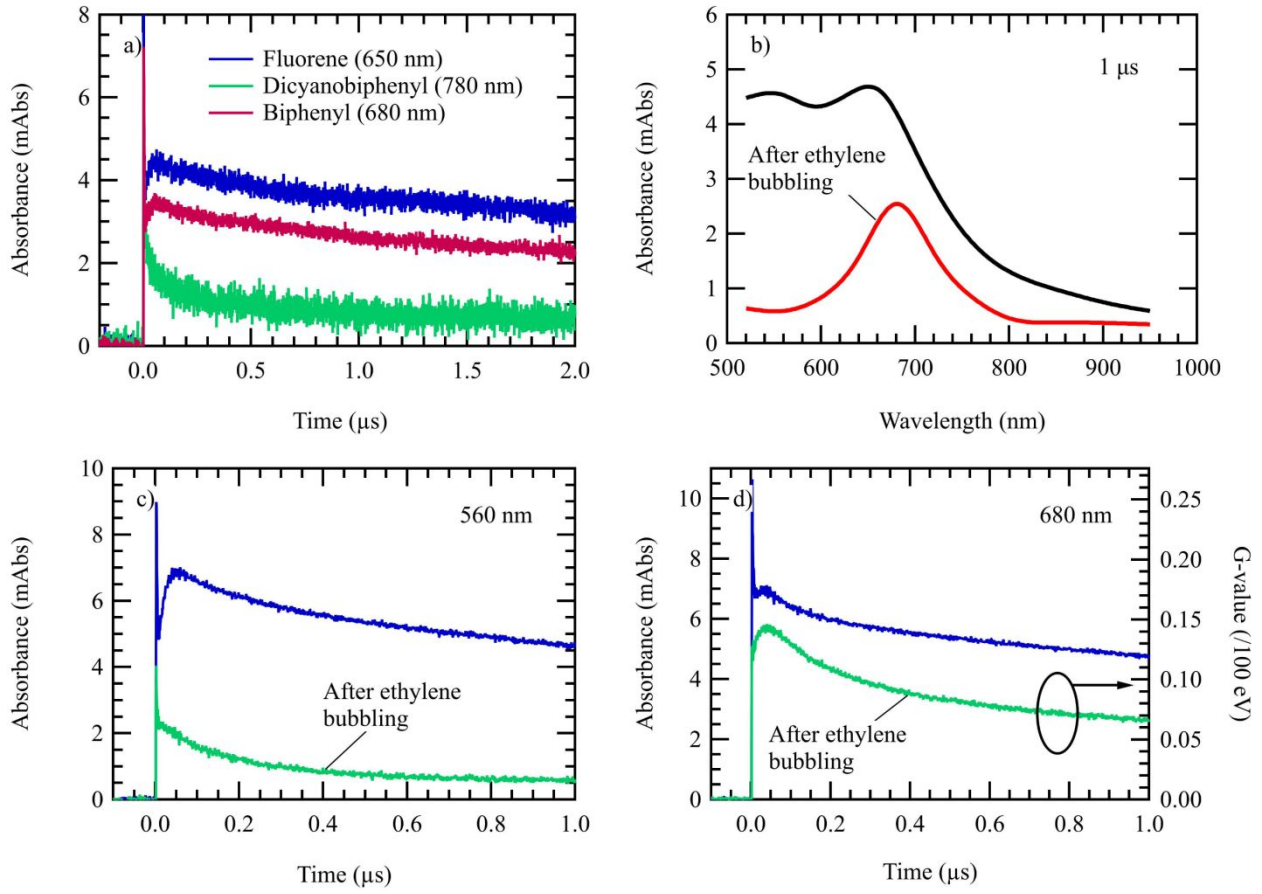

Fig 3 a) Transient absorption following PR in $CDCl_3$ with dose of 27.0 Gray at wavelengths where the solute cation absorbs with solutes at 1 mM. b) Absorption spectra at 1 μs following PR in $CDCl_3$ for solution with 1 mM of biphenyl without (black) and with (red) bubbling with ethylene. Transient absorption of solutions from b) shown without (blue) and with (green) ethylene bubbling at c) 560 nm and d) 680 nm. Dose in figures b) to d) = 35.4 Gray. All path lengths are 0.5 cm and all solutions are Ar-bubbled unless otherwise stated.

CCl_4 either.[3] The explanation for this behavior is that the observed spectra in $CHCl_3$ and CCl_4 are dominated by the Cl atom complex with the biphenyl. Cl atoms will live longer in $CHCl_3$ or CCl_4 compared to 1,2-DCE due to a lower or non-existent concentration of available H atoms to abstract respectively. DFT calculations predict that ethene will form a very strong complex with Cl atom (C-Cl bond length = 1.92 Å), much like amylene stabilizers, commonly added to chloroform, might. We therefore bubbled the solution with ethene and found that the absorption from the complex disappeared leaving only the biphenyl radical cation (red spectrum). A similar effect can be achieved using carbon disulfide (see Fig S9 in ESI†), which also strongly complexes Cl atoms.[36] Without ethene Fig 3c shows a growth of absorption at 560 nm that can be attributed to formation of the (Cl, biphenyl) complex. Addition of ethene prevents the 560 nm growth but there was still a growth at 680 nm (Fig 3d), where biphenyl cation absorbs. The pseudo first order rate constant for the biphenyl cation growth is 5.7×10^7 s^{-1}, indicating oxidation by a longer-lived species than the solvent radical cation which decays faster ($k_d \geq 10^8$ s^{-1}). This growth is most likely from the bimolecular hole transfer reaction from ethene radical cation or its dimer to biphenyl. We can therefore not conclusively attribute the additional biphenyl cations to oxidation by CCl_3^+. We were unable to find a Cl atom scavenger that would not also intercept holes from the solvent. Computations predict that the molecule tricyanoethene would be able to remove the Cl atom complex and not interfere with the hypothesized $CDCl_3^{+\bullet}$ fragmentation because its IP would be too high to be oxidized. Unfortunately, we were unable to obtain tricyanoethene from commercial suppliers.

For solutes with an IP less than or equal to that of p-terphenyl, oxidation by Cl atom occurs, setting a lower limit for solutes where oxidation by a fragment cation might be observed free from growths fed by other species. The redox window for performing this experiment is therefore only ~ 200 mV and we have not found a solute in this region without an overlapping absorption from the complex. While we were not able to directly detect CCl_3^+ through these experiments, the energetic arguments described above and the reported production of CCl_4, that can be prevented with hole scavengers,[20] still make CCl_3^+ the strongest candidate for the cation formed by fragmentation of $CDCl_3^{+\bullet}$.

Table 2. Summary of evidence for formation of solute cations in $CDCl_3$ following pulse radiolysis. Solutes above the dashed line showed no evidence being oxidized. Evidence includes an effect on the yield of radical cations of dicyanobiphenyl (lower IP probe solute) through addition of 100 mM of high-IP solutes, the observation of the solute cation and/or reaction with the visible absorption band present in the neat solvent after PR.

Test Solute	Calc. IP in gas phase (eV)[a]	Calc. absolute E^o in chloroform (V)[b]	Est. E^o in chloroform vs Fc/Fc+ (V)[c]	Change in probe yield? (factor)[d]	See test solute cation absorption?[e]	React with visible solvent species?[f]
$(CF_3)_3$ triazene	11.13	9.37	4.31	-	No	No
$(C_3F_7)_3$ triazene	10.84	9.38	4.32	No[g]	No	No
Hexachloroethane	10.61	8.98	3.92	No[g]	No	No
Fumaronitrile	10.76	8.75	3.69	Yes (0.3)	No	Yes
Dichloroethane	10.49	8.67	3.61	Yes (5.0)	Yes	Yes
Carbon tetrabromide	10.05	8.25	3.19	Yes (0.6)	Possible*	Overlap
Pentane	9.88	8.13	3.07	Yes (1.3)	No	Yes
Carbon disulfide	10.12	8.06	3.00	Yes (7.2)	Yes	Overlap
Hexafluorobenzene	9.84	7.90	2.84	Yes (3.3)	No	Yes
Cyclohexane	9.50	7.67	2.61	Yes (1.1)	No	Yes
Decane	9.10	7.73	2.67	Yes (2.3)	Yes	Overlap
Decafluorobiphenyl	9.25	7.62	2.56	Yes (5.2)	Yes	-
2,3 dimethyl butane	9.29	7.55	2.49	Yes (0.1)	No	Yes
Benzene	9.03	7.22	2.16	No[h]	Yes	-
Dicyanobiphenyl (probe)	8.63	7.06	2.00	-	-	-

Table notes: a) IP calculated with DFT using enthalpy as in Table 1, where the calc. IP for $CHCl_3$ is 11.11 eV b) Calculated absolute E^o as defined in Table 1 (absolute $E^o(CHCl_3)$ = 9.15 V). c) Calculated E^o vs Fc/Fc^+ as described in Table 1 (est. $E^o(CHCl_3)$ = 4.09 V vs Fc/Fc^+). d) Ratio of CN2BP radical cation at 500 ns after electron pulse with or without 100 mM of "test" solute e) Was there direct evidence of solute radical cation formation observed as a new transient absorption spectrum? f) Did the solvent absorption decay faster with the solute present? In some cases it is less clear due to the solute radical cation overlapping g) Matches dicyanobiphenyl (1 mM) cation decay h) Matches test solute (100 mM) decay so no hole transfer to "probe" solute. *A broad absorption centered ~ 550 nm might be the CBr_4 cation, but despite have a lifetime of 30 ns, it reduced the yield of the "probe" dicyanobiphenyl cations suggesting its lifetime could not be as long as 30 ns.

III. Making cations of high IP solutes

To further investigate the cause of the unusually short lifetime of $CDCl_3^{+\bullet}$, the lifetimes of a series of cations of high IP solutes were studied in $CDCl_3$. Due to the absence of a detectable cation absorption in most of these solutes, a method involving two solutes was devised to infer if a cation was formed and how long it lived. A probe solute with a lower IP was added at 1 mM, which, as shown in Fig 2b, will capture only ~5 – 15 % of available homogeneous ions from the $CDCl_3^{+\bullet}$ (G = 0.005 – 0.014 ions /100 eV at 500 ns). By adding 100 mM of various high IP test solutes which will capture >90% of available $CDCl_3^{+\bullet}$ first, we can infer whether a long-lived cation of the test solute was formed by looking for an increase in the yield of the probe solute cation later at 500 ns. Table 2 summarizes the findings of this experiment. Dicyanobiphenyl (IP_{calc} = 8.63 eV), which has a strong cation absorption at 780 nm, was used as the probe solute.

The results, shown in Table 2, suggest that $CDCl_3^{+\bullet}$ is not unique in being short-lived. Fumaronitrile, pentane, carbon tetrabromide, cyclohexane, and 2,3-dimethyl butane likely have similar or shorter lifetimes than $CDCl_3^{+\bullet}$ as they either reduce or maintain a similar yield of dicyanobiphenyl cations. Of the solutes tested, cations of dichloroethane, carbon disulfide, hexafluorobenzene, decafluorobiphenyl and decane appeared to have significantly longer lifetimes than $CDCl_3^{+\bullet}$, increasing the yield of the probe cation by factors between 2 and 7.

Cations formed from benzene (IP_{calc} = 9.03 eV) were unable to oxidize dicyanobiphenyl (IP_{calc} = 8.63 eV) as seen in Table 2, probably because benzene is known to form a dimer cation. An estimate of the dissociation energy of the dimer cation in the gas phase at 300 K is 0.66 ± 0.04 eV[47], and being at 100 times higher concentration than dicyanobiphenyl in our experiment, benzene dimer cation would not transfer a hole to dicyanobiphenyl.

It appears that rapid fragmentation, similar to that of $CDCl_3^{+\bullet}$, occurs for radical cations of many molecules in $CDCl_3$. Whether the surrounding $CDCl_3$ molecules speed up this decay through reactions similar to equation 16 is yet to be determined. Another important conclusion is that we were able to observe evidence (either *directly* as the observation of cation, or *indirectly* as a change in the yield of "probe" cations) of cations being formed for solutes with predicted oxidation potentials up to +3.7 V vs Fc/Fc+ which is just 0.4 V below the calculated oxidation potential of $CDCl_3$ itself.

IV. Assignment of visible absorption band

Finally, we seek to assign the visible absorption band in $CDCl_3$ following PR. Fig 4a shows transient absorption spectra for neat $CDCl_3$, normalized by dose and path length. We hypothesized that the broad visible absorption is dominated by the chloroform parent cation. To test the hypothesis that the broad, visible absorption band is due to $CDCl_3^{+\bullet}$, we investigated the effect of various solutes on the decay

kinetics at 740 nm, in the red part of this band, as shown in Fig 4b. At 740 nm absorptions from cations of the solutes used in Fig 4 is small. Every solute that showed direct, or indirect evidence of being oxidized by $CDCl_3^{+\bullet}$ in section III (see Table 2) also caused an increase in the decay rate of the solvent band at 740 nm. Hexachloroethane showed neither evidence of cation formation nor caused any change in the solvent band decay kinetics. We find that solutes with an oxidation potential similar to or larger than hexachloroethane cannot be oxidized by $CDCl_3^{+\bullet}$ (see Table 2).

Given this evidence that the solvent band is due to $CDCl_3^{+\bullet}$ we tried a second method to estimate the decay rate of $CDCl_3^{+\bullet}$ from fragmentation (k_d). This method compared the kinetics of the $(CS_2)_2^{+\bullet}$ decay with that of the solvent band (Fig 4c). If k_d were 0, after hole transfer to CS_2 is complete at ~ 1 ns we might expect $(CS_2)_2^{+\bullet}$ to decay with the same kinetics as the solvent cation, but we see the solvent band go away faster. To estimate the rate constant, k_d, for the additional decay pathway of the solvent cation, we multiplied the $(CS_2)_2^{+\bullet}$ cation kinetic trace (green, Fig 4c) by an exponential decay, $\exp(-k_d t)$, to obtain a best fit (blue trace) to the solvent kinetics (black trace). To obtain the fit, a constant factor, ε_{ratio}, was also required to account for the different extinction coefficient of $CDCl_3^{+\bullet}$ compared to $(CS_2)_2^{+\bullet}$. We obtained $\varepsilon_{ratio} = 0.67$ and $k_d = (3.2 \pm 0.8) \times 10^8$ s^{-1} giving a $CDCl_3^{+\bullet}$ fragmentation lifetime of ~3 ns. This approach for estimating k_d assumes that the recombination kinetics of $CDCl_3^{+\bullet}$ with chloride counterion is similar to that of $(CS_2)_2^{+\bullet}$ and thus contains uncertainties. We estimate that the diffusion coefficients for $CDCl_3^{+\bullet}$ and $(CS_2)_2^{+\bullet}$ would differ by up to 25%, based on mobilities of monomer and dimer ions[48] which is the largest source of error using this approach. With the estimate of ε_{ratio} we determined an extinction coefficient $\varepsilon(CDCl_3^{+\bullet}) = 4{,}430$ $M^{-1}cm^{-1}$ at 740 nm. This estimate also uses a factor of 0.85 for the $(CS_2)_2^{+\bullet}$ absorption at 740 nm compared to its peak at 690 nm, where $\varepsilon((CS_2)_2^{+\bullet}) = 7{,}775$ $M^{-1}cm^{-1}$ (from Fig 1a).

TD-DFT calculations in Fig S10 in ESI† support our assignment showing a broad absorption in the vis/nearIR, peaking ~780 nm for $CHCl_3^{+\bullet}$ with an extinction coefficient ~ 3,000 $M^{-1}cm^{-1}$. The calculations also predict that none of the other possible species, CCl_3^+, $CCl_3^\bullet$, $CHCl_2^+$, $CHCl_2^\bullet$, or CCl_2^+ absorb at wavelengths longer than 300 nm.

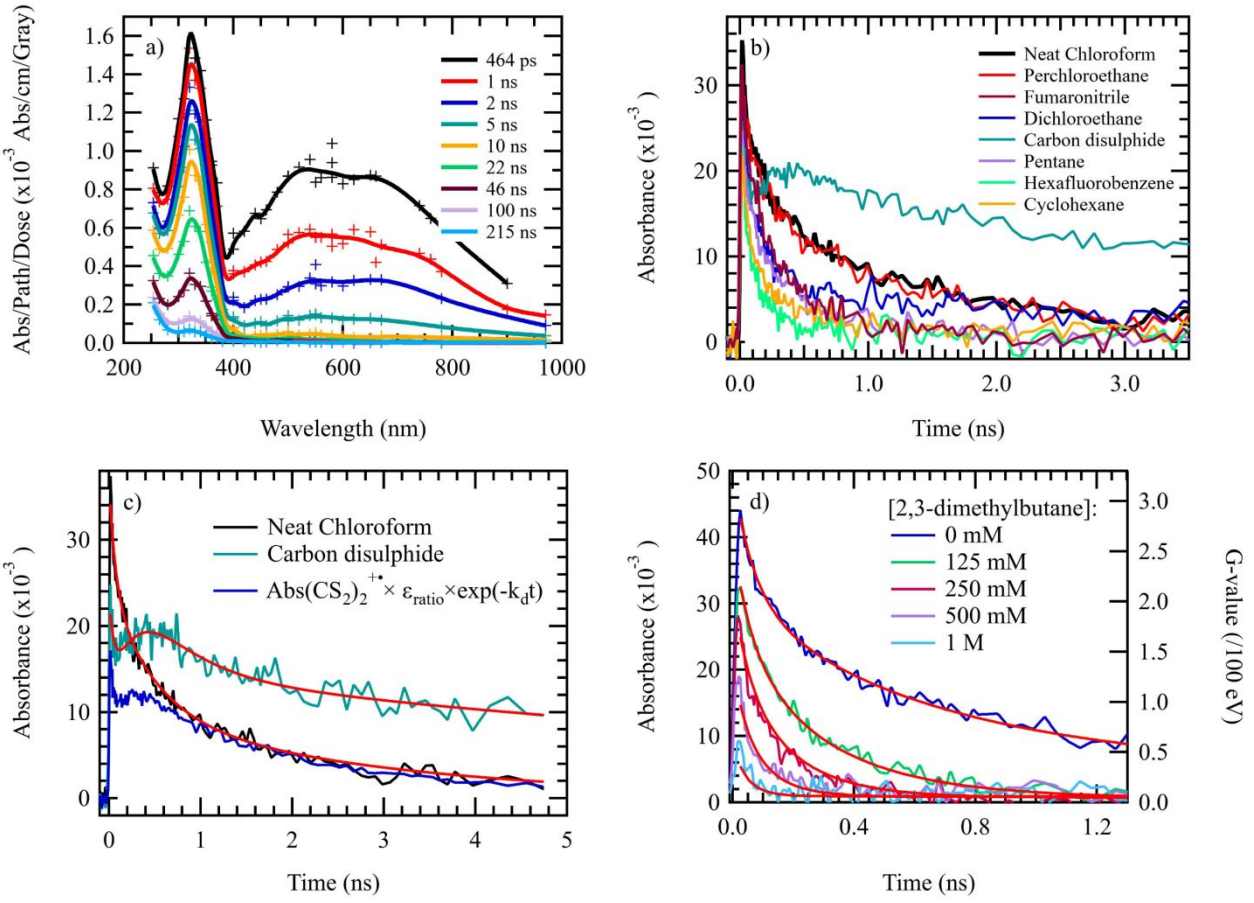

Fig 4 a) Transient absorption spectra normalized by dose and path length in $CDCl_3$ following PR. b) Transient absorption following PR at 740 nm with dose of 38.8 Gray in 0.5 cm path length for solutions of various high IP solutes at 200 mM in $CDCl_3$. c) Data from Fig 4b) with fits for bimolecular hole transfer mechanism, and dimerization to form $(CS_2)_2^{+\bullet}$. The blue trace is the best fit to the solvent band by modifying the $(CS_2)_2^{+\bullet}$ absorption as described in the text. d) Transient absorption following PR at 740 nm with dose of 44.1 Gray in 0.5 cm path length for 2,3-dimethylbutane at various concentrations in $CDCl_3$. Global fits shown in red with $k_{att} = 1.72 \times 10^{10}$, $M^{-1}s^{-1}$ and q = 1.8 M^{-1}.

To further confirm the assignment of the visible band to $CDCl_3^{+\bullet}$, we investigated whether its faster decay, when a solute is present, corresponded to the growth kinetics of the solute cation. Again, we use the data in Fig 4c due to the ability to see a clear growth of $(CS_2)_2^{+\bullet}$. Firstly, the absorption in the neat solvent (black trace) is fitted to three fractions with different exponential decays as a model for the decay of geminate and homogeneous ions. Then the trace for the solution containing 200 mM CS_2 (green trace) was fitted under the assumption of hole transfer from the solvent species to form $CS_2^{+\bullet}$ followed by dimerization to the observable $(CS_2)_2^{+\bullet}$ dimer cation. As shown with the red traces in Fig 4c, the model fits the kinetic traces well using a ratio of $(CS_2)_2^{+\bullet}$ to $CHCl_3^{+\bullet}$ extinction coefficient already determined as ε_{ratio} = 0.67. The hole transfer required a faster-than-diffusion component to fit the 30% reduction in the solvent band at the earliest time that we could resolve (~15 ps). The same phenomenon has recently been observed as "step" increases in solute cation absorptions in chloroform.[6] The loss of solvent cation due to "step" capture is modelled as exp(-*q**[*solute*]). The best fit came from a combination of q = 1.13 ± 0.06 M^{-1} and k_{att} = (2.4 ± 0.15) × 10^{10} $M^{-1}s^{-1}$.

To improve upon the estimated k_{att}, Fig 4d shows a global fit of the visible band transient absorption for different concentrations of 2,3-dimethylbutane in $CDCl_3$. Again, matching the observed shape of the transient absorption required a "step" capture component. The whole dataset could be fitted with q = 1.80 ± 0.04 M^{-1} and k_{att} = (1.72 ± 0.03) × 10^{10} $M^{-1}s^{-1}$. While this rate constant is for hole attachment to 2,3-dimethylbutane rather than CS_2, taken together with the previous paragraph, it is suggestive that ~2 × 10^{10} $M^{-1}s^{-1}$ is a reasonable estimate diffusion-controlled hole transfer to a generic solute in $CDCl_3$.

The right axis in Fig 4d shows the G-value for solvent cations based on the estimated extinction coefficient of the chloroform cation from the fit in Fig 4c. We estimate the G-value for $CDCl_3^{+\bullet}$ at t = 15 ps to be 2.8 ± 0.2 ions/100 eV and likely > 3.0 ions/100eV at t = 0. This is larger than that estimated in Fig 1b (2.3 ions/100 eV) from the CS_2 dimer cation which could be due to ion recombination happening before CS_2 cations have time to dimerize and become observable. A value of $G(CDCl_3^{+\bullet})$ > 3.0 ions/100 eV gets closer to the literature values for the primary neutral radicals of $G(Cl^{\bullet})$ = 4.6[19] and 4.8 ± 0.1[26] and $G(CHCl_2^{\bullet})$ = 4.8.[19], 5.0 [20,21] and 5.9 ± 0.4.[26] This suggests that most 'primary' radicals are formed by ionizations.

A G value of 3.0 ions/100eV for primary ions already accounts for a loss of chloroform with of 9.0 molecules/100 eV due the radical anion fragmentation and subsequent radical reactions (equations 2, 5 and 6). Fragmentation of $CDCl_3^{+\bullet}$ to CCl_3^+ (eqn 16) followed by recombination with Cl^- to make CCl_4 (eqn 18) would result in a net additional consumption of two $CDCl_3$ equal to 2 × $G(CCl_4)$ = 1.8 molecules/100 eV[20] compared to if fragmentation had not happened. Ion fragmentation and subsequent radical reactions therefore appear to be able to account for most of the chloroform decomposition $G(-CDCl_3)_{ions}$ = 10.8 molecules/100 eV, falling just short of the reported total $G(-CHCl_3)$ = 12 molecules/100 eV.[18]

While some uncertainty remains, a reasonable interpretation of these G-values is that some $CDCl_2^{\bullet}$ and $Cl^{\bullet}$ are also formed either by $CDCl_3$* decomposition (eqn 4), or geminate recombination that occurs on the sub 15 ps timescale. For either process, the G value would be < 1.8 species/100eV to be consistent with our data and existing literature. Either of these mechanisms could account for larger reported G values for radical formation and $CHCl_3$ consumption than we can account for due to observable ionizations alone.

Conclusions

Pulse radiolysis of liquid $CDCl_3$ at room temperature produces $CDCl_3^{+\bullet}$ which can oxidize solutes having oxidation potentials up to an estimated +3.7 V vs Fc/Fc+, extending typical voltammetry oxidation limits by over a volt.

$CDCl_3^{+\bullet}$ is formed with a yield G = 2.8 ± 0.2 ions/100 eV at t = 15 ps and likely to be > 3 ions/100 eV at t = 0. Charge recombination is extremely rapid with the G-value dropping to below 1.0 ion/100 eV by 1 ns and below 0.1 ions / 100 eV by 500 ns. Two independent experiments suggest that $CDCl_3^{+\bullet}$ has an intrinsic lifetime of 6 ± 3 ns that is competitive with ion recombination, causing a $CDCl_3^{+\bullet}$ to disappear almost entirely by 20 ns. Our data, in the context of existing literature, is consistent with the process being fragmentation of $CDCl_3^{+\bullet}$ to form CCl_3^+ which ultimately forms CCl_4 through recombination with Cl^-. DFT studies showed this fragmentation to be energetically downhill when surrounding solvent molecules participate. Our results suggest that while some radicals are formed by decomposition of $CDCl_3$ excited states, the majority of the radiation chemistry in chloroform is initiated by ionizations despite suggestions to the contrary.[18]

Data presented here strongly support the identification of the broad absorption in the visible region in neat $CDCl_3$ following pulse radiolysis as $CDCl_3^{+\bullet}$. Its unusual kinetics are due to the competition between ion recombination and fragmentation.

Chloroform can therefore be used to make and study free ions of high IP solutes with pulse radiolysis. For the maximum yield of captured free ions, the solute should be present at ≥ 100 mM or a second, higher IP solute added at that concentration to outcompete the fragmentation. Chloroform is ideal for studying fast processes and the highest IP solutes due to it generally being a better solvent and having a higher IP. Chloroform may therefore be an excellent choice for studying high IP, short-lived cations and data presented here shows how lifetimes of solute cations could be investigated with this technique.

In order to clearly study cations of high IP solutes, ethenes can be used to scavenge the $Cl^{\bullet}$ atoms that otherwise form strongly absorbing complexes in the visible part of the spectrum with most solutes following ion recombination.

For solutes with an IP lower than that of p-terphenyl, it cannot be guaranteed that all the observed ions are free ions because recombination with Cl^- forms stable ion pairs like (p-terphenyl$^{\bullet+}$,Cl^-). Absorption spectra of these ion pairs are similar to those of the free cations. For PR in chloroform, it can therefore only be guaranteed that observed solute radical cations are *free* if the solute oxidation potential is between ~ 1.0 and 3.7 V vs Fc/Fc+. While $CHCl_3^{+\bullet}$ and $Cl^{\bullet}$ can oxidize solutes, other radicals or cations such as CCl_3^+, $CHCl_2^+$, $CCl_3^{\bullet}$ and $CHCl_2^{\bullet}$ could provide additional agents for oxidation of solutes having low oxidation potentials.

Conflicts of interest

There are no conflicts to declare.

Acknowledgements

This material is based upon work supported by the U.S. Department of Energy, Office of Science, Office of Basic Energy Sciences, Division of Chemical Sciences, Geosciences & Bioscience through Grant DE-SC0012704, including use of the LEAF and Van de Graaff facilities of the BNL Accelerator Center for Energy Research.

Notes and references

1 A. J. Bard and L. R. Faulkner, *Electrochemical Methods: Fundamentals and Applications, 2nd Edition*, Wiley Textbooks 2000.
2 N. Elgrishi, K. J. Rountree, B. D. McCarthy, E. S. Rountree, T. T. Eisenhart and J. L. Dempsey, *J. Chem. Educ.*, 2018, **95**, 197-206.
3 S. Arai, H. Ueda, R. F. Fireston and L. M. Dorfman, *J. Chem. Phys.*, 1969, **50**, 1072-1077.
4 H. D. Burrows, M. D. Miguel, A. P. Monkman, L. E. Horsburgh, I. Hamblett and S. Navaratnam, *J. Chem. Phys.*, 2000, **112**, 3082-3089.
5 H. D. Burrows, J. S. de Melo, M. Forster, R. Guntner, U. Scherf, A. P. Monkman and S. Navaratnam, *Chem. Phys. Lett.*, 2004, **385**, 105-110.
6 A. R. Cook, M. J. Bird, S. Asaoka and J. R. Miller, *J. Phys. Chem. A*, 2013, **117**, 7712-7720.
7 S. G. Lias, *"Ionization Energy Evaluation"*, National Institute of Standards and Technology, Gaithersburg MD, 208992019.
8 S. Creager, in *Handbook of Electrochemistry*, ed. C. G. Zoski, Elsevier, Amsterdam 2007.
9 M. Washio, S. Tagawa and Y. Tabata, *Radiat. Phys. Chem.*, 1983, **21**, 239-243.
10 M. Washio, S. Tagawa, K. Furuya, N. Hayashi and Y. Tabata, *Radiat. Phys. Chem.*, 1989, **34**, 533-537.
11 H. D. Burrows, T. J. Kemp and Greatore.D, *J. Phys. Chem.*, 1972, **76**, 20-26.
12 R. E. Buhler, A. S. Domazou and Y. Katsumura, *J. Phys. Chem. A*, 1999, **103**, 4986-4992.
13 V. I. Borovkov, *J. Phys. Chem. B*, 2017, **121**, 9422-9428.
14 M. A. Quadir, T. Azuma, A. S. Domazou, Y. Katsumura and R. E. Bühler, *J. Phys. Chem. A*, 2003, **107**, 11361-11370.
15 C.-R. Wang, K. Drew, T. Luo, M.-J. Lu and Q.-B. Lu, *J. Chem. Phys.*, 2008, **128**, 041102.
16 A. Saeki, N. Yamamoto, Y. Yoshida and T. Kozawa, *J. Phys. Chem. A*, 2011, **115**, 10166-10173.
17 A. O. Allen, *Yields of free ions formed in liquids by radiation*, National Bureau of Standards, United States, 1976.
18 M. J. M. Abadie, *Radiat. Phys. Chem.*, 1982, **19**, 68-71.
19 H. R. Werner and R. F. Firestone, *J. Phys. Chem.*, 1965, **69**, 840-849.
20 J. N. Baxter and N. E. Bibler, *J. Chem. Phys.*, 1970, **53**, 3444-3450.
21 N. E. Bibler, *J. Phys. Chem.*, 1971, **75**, 2436-2442.
22 F. P. Abramson and R. F. Firestone, *J. Phys. Chem.*, 1966, **70**, 3596-3605.
23 F. J. Johnston, T.-H. Chen and K. Y. Wong, *J. Phys. Chem.*, 1961, **65**, 728-730.
24 T. H. Chen, K. Y. Wong and F. J. Johnston, *J. Phys. Chem.*, 1960, **64**, 1023-1025.
25 A. Henglein and H. Mohehauer, in *Z. Phys. Chem.*1958, vol. 18, p. 43.
26 M. Ottolenghi and G. Stein, *Radiat. Res.*, 1961, **14**, 281-290.
27 N. E. Bibler and M. L. Hyder, *Nature*, 1968, **219**, 374-375.
28 J. E. Chateauneuf, *J. Am. Chem. Soc.*, 1990, **112**, 442-444.
29 J. E. Chateauneuf, *Chem. Phys. Lett.*, 1989, **164**, 577-580.
30 Y. Katsumura and R. E. Bühler, *Int. J. Radiat. Appl. Instrum. Part C*, 1989, **34**, 543-545.
31 F. Abou-Chahine, T. J. Preston, G. T. Dunning, A. J. Orr-Ewing, G. M. Greetham, I. P. Clark, M. Towrie and S. A. Reid, *J. Phys. Chem. A*, 2013, **117**, 13388-13398.
32 M. Washio, Y. Yoshida, N. Hayashi, H. Kobayashi, S. Tagawa and Y. Tabata, *Radiat. Phys. Chem.*, 1989, **34**, 115-120.
33 H. Miyasaka, H. Masuhara and N. Mataga, *Chem. Phys. Lett.*, 1985, **118**, 459-463.
34 G. Zhang and J. K. Thomas, *Photochem. Photobiol.*, 2006, **82**, 158-162.
35 R. E. Buhler and M. Ebert, *Nature*, 1967, **214**, 1220-1221.
36 J. E. Chateauneuf, *J. Am. Chem. Soc.*, 1993, **115**, 1915-1921.
37 G. A. Russell, A. Ito and D. G. Hendry, *J. Am. Chem. Soc.*, 1963, **85**, 2976-2983.
38 J. F. Wishart, A. R. Cook and J. R. Miller, *Rev. Sci. Instrum.*, 2004, **75**, 4359-4366.
39 A. R. Cook and Y. Z. Shen, *Rev. Sci. Instrum.*, 2009, **80**, 1-7.
40 M. J. Frisch, G. W. Trucks, H. B. Schlegel, G. E. Scuseria, M. A. Robb, J. R. Cheeseman, G. Scalmani, V. Barone, B. Mennucci, G. A. Petersson, H. Nakatsuji, M. Caricato, X. Li, H. P. Hratchian, A. F. Izmaylov, J. Bloino, G. Zheng, J. L. Sonnenberg, M. Hada, M. Ehara, K. Toyota, R. Fukuda, J. Hasegawa, M. Ishida, T. Nakajima, Y. Honda, O. Kitao, H. Nakai, T. Vreven, J. A. Montgomery, Jr., J. E. Peralta, F. Ogliaro, M. Bearpark, J. J. Heyd, E. Brothers, K. N. Kudin, V. N. Staroverov, R. Kobayashi, J. Normand, K. Raghavachari, A. Rendell, J. C. Burant, S. S. Iyengar, J. Tomasi, M. Cossi, N. Rega, N. J. Millam, M. Klene, J. E. Knox, J. B. Cross, V. Bakken, C. Adamo, J. Jaramillo, R. Gomperts, R. E. Stratmann, O. Yazyev, A. J. Austin, R. Cammi, C. Pomelli, J. W. Ochterski, R. L. Martin, K. Morokuma, V. G. Zakrzewski, G. A. Voth, P. Salvador, J. J. Dannenberg, S. Dapprich, A. D. Daniels, Ö. Farkas, J. B. Foresman, J. V. Ortiz, J. Cioslowski and D. J. Fox, Gaussian, Inc., Wallingford CT2009, vol. Revision D.01.
41 T. Sumiyoshi, M. Nakayama, R. Fujiyoshi and S. Sawamura, *Radiat. Phys. Chem.*, 2005, **74**, 317-322.

42 C. P. Kelly, C. J. Cramer and D. G. Truhlar, *J. Phys. Chem. B*, 2006, **110**, 16066-16081.
43 C. P. Kelly, C. J. Cramer and D. G. Truhlar, *J. Phys. Chem. B*, 2007, **111**, 408-422.
44 C. J. Cramer, *Essentials of Computational Chemistry: Theories and Models, 2nd Edition*, Wiley 2004.
45 S. Fukuzumi, K. Ohkubo, H. Imahori and D. M. Guldi, *Chem. Eur. J.*, 2003, **9**, 1585-1593.
46 I. R. Gould, D. Ege, J. E. Moser and S. Farid, *J. Am. Chem. Soc.*, 1990, **112**, 4290-4301.
47 J. R. Grover, E. A. Walters and E. T. Hui, *J. Phys. Chem.*, 1987, **91**, 3233-3237.
48 S. K. Lim, M. E. Burba and A. C. Albrecht, *J. Phys. Chem.*, 1994, **98**, 9665-9675.

ToC

We show that pulse radiolysis in chloroform enables the creation and study of radical cations beyond traditional electrochemical windows.